Civil Engineering
Engenharia Civil

Vibration behavior of thin-walled steel members subjected to uniform bending

http://dx.doi.org/10.1590/0370-44672017710168

Andréa Gonçalves Rodrigues das Dôres
http://orcid.org/0000-0003-2187-7082
Engenheira Civil
Ouro Preto - Minas Gerais - Brasil
rgandrea@yahoo.com.br

Dinar Camotim
Professor-Catedrático
Universidade de Lisboa
Instituto Superior Técnico, DECivil
Lisboa - Portugal
dcamotim@civil.ist.utl.pt

Pedro Borges Dinis
Professor-Auxiliar
Universidade de Lisboa
Instituto Superior Técnico, DECivil
Lisboa - Portugal
dinis@civil.ist.utl.pt

Marcilio Sousa da Rocha Freitas
Professor-Titular
Universidade Federal de Ouro Preto - UFOP
Escola de Minas
Departamento de Engenharia Civil
Ouro Preto - Minas Gerais - Brasil
marcilio@em.ufop.br

Abstract

This article reports the results of an investigation on the effects of internal moments on the vibration behavior of thin-walled steel members. The analyses are based on the Generalized Beam Theory (GBT), a thin-walled bar theory accounting for cross-section in-plane deformations – its main distinctive feature is the representation of the member deformed configuration by means of a linear combination of cross-section deformation modes, multiplied by their longitudinal amplitude functions. The study concerns a simply supported T-section (with unequal flanges) members exhibiting a wide range of lengths and subjected to uniform internal moment diagrams – their magnitudes are specified as percentages of the corresponding critical buckling values. After providing a brief overview of the main concepts and procedures involved in performing a GBT-based structural analysis, the vibration behavior of load-free and loaded T-section members is addressed – the influence of the applied loadings is assessed in terms of (i) the fundamental frequency difference and (ii) the change in the corresponding vibration mode shape. For validation purposes, some GBT results are compared with values yielded by shell finite element analysis performed in the code ABAQUS (Simulia, 2008).

Keywords: thin-walled members, Generalized Beam Theory (GBT), vibration of loaded beams, local, distortional and global vibration.

1. Introduction

It is well known that, due to the high slenderness of their walls, thin-walled members exhibit responses that may be governed by phenomena involving local and/or distortional deformations of their cross-sections. Moreover, it is a common practice to analyze their vibration behavior under the (approximate) assumption that they are not subjected to any loading. *i.e.,* load-free. However, structural members are invariably subjected to loadings of more or less significant magnitude and, therefore, the associated geometrically non-linear effects (local, distortional or global) may have some impact on their natural vibration frequencies and mode shapes.

Over the last decades, several studies have been published concerning the vibration behavior of thin-walled members acted upon by axial forces (*e.g.,* de Borbón and Ambrosini, 2010; Vo and Lee, 2011) and/or bending moments (*e.g.,* Shih *et al.,* 1986; Joshi and Suryanarayan, 1989, 1991; Pavlović *et al.,* 2007; Mohri *et al.,* 2008; Magnucka-Blandzi, 2009; Vo and Lee, 2010, 2013; Motamarri and Suryanarayan, 2012; Talimian and Vörös, 2013; Kashani *et al.,* 2014; Verma, 2015). Regarding the second group of publications, one must especially mention the contribution of (i) Shih *et al.* (1986), related to the analytical solution of the flexural vibration of long simply-supported beams subjected to their own weight, (ii) Talimian and Vörös (2013) investigated the dynamic stability of a thin-walled beam subjected to a time periodic gradient bending moment, and (iii) Verma (2015) analysed the flexural-torsional vibration of a thin-walled beam due to the combined action of bending moment and torque.

However, the vast majority of these works are restricted to members vibrating in *global* modes, i.e., involving exclusively bending and/or torsional deformations. Only a few (and quite recent) publications deal with the local and distortional vibration of loaded thin-walled members – most of them concerning members under axial force, i.e., columns (*e.g.,* Okamura and Fukasawa, 1998; Ohga *et al.,* 1998) and only a few concerning thin-walled members subjected to bending (*e.g.,* Urbaniak and Kubiak, 2011).

The Generalized Beam Theory (GBT) was originally developed by

Schardt (1966) and may be viewed as an extension of Vlasov's classical bar theory (Vlasov, 1961) that incorporates genuine folded-plate concepts and, thus, is able to take into account in-plane (local) cross-section deformations. Moreover, the member deformed configuration is expressed as a linear combination of a set of pre-determined cross-section deformation modes – due to this rather unique modal nature, the application of GBT is considerably more versatile and computationally efficient than similar finite strip or shell finite element analyses. Indeed, it has been recently shown that GBT provides a rather powerful, elegant and clarifying tool to investigate a wealth of structural problems involving thin-walled prismatic members (*e.g.,* Silvestre and Camotim, 2002; Camotim *et al.,* 2010).

Taking advantages of the exclusive modal decomposition features of GBT, Schardt and Heinz (1991) study the local, distortional and global vibration behavior of load-free isotropic thin-walled members. Since then, new formulations have been extensively developed and implemented by Silvestre and Camotim (2016, 2006a, 2012), and Bebiano *et al.* (2008, 2013) to analyze the vibration behavior of thin-walled members acted upon by loadings that may include combinations of axial force and uniform or non-uniform bending – a study dealing with the influence of pure bending in steel I-section beams was also reported by Camotim *et al.* (2007). However, it must be said that no investigation was carried for intermediate-to-long beams, with asymmetric cross-sections, that buckle in distortional modes – the present work aims at providing a first contribution towards filling this gap.

The objective of this work is to present a GBT-based study concerning the local, distortional and global vibration behavior of thin-walled members acted upon by a uniform major-axis bending moment. The analyses are carried out for simply supported T-section (with unequal flanges) beams exhibiting a wide length range and subjected to several loading levels, defined as percentages of the corresponding critical bifurcation values. The influence of the loading is assessed through the comparison relatively to the load-free case of the (i) natural frequency values and (ii) vibration mode shapes. The results presented and discussed are validated by means of values and mode shapes provided by numerical analyses performed with the code ABAQUS (Simulia, 2008), adopting fine meshes of four-node isoparametric shell (S4) elements (length-to-width ratio close to 1) to discretize the columns.

2. Generalized beam theory – brief overview

As mentioned earlier, the GBT is a one-dimensional bar theory that expresses/discretizes the member deformed configuration as a linear combination of cross-section deformation modes multiplied by the corresponding (modal) amplitude functions. Its application involves the performance of two main tasks, namely (i) a *cross-section analysis* and (ii) *a member analysis* – a very brief overview of this theory is presented next (a complete account can be found, e.g., in Silvestre and Camotim, 2002a) and, for illustrative purposes, one considers the member depicted in Fig. 1(a) – also shown is the member global coordinate system *X–Y–Z* (longitudinal, major and minor axis). Note that, in each wall, a local coordinate system (*x-s-z*) is adopted, where *x* and *s* define the corresponding mid-surface (longitudinal and transverse directions) and *z* is measured along the wall thickness (*e*) during time (*t*).

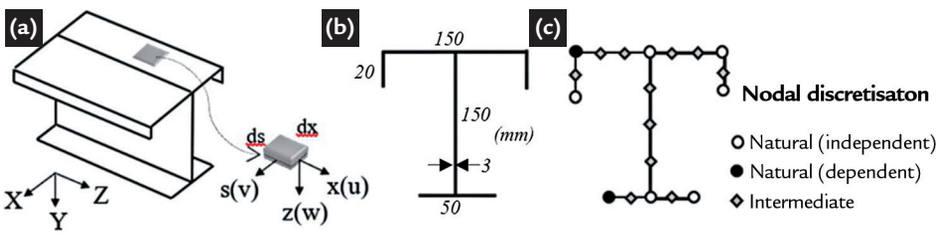

Figure 1
T-section: (a) Coordinate system and displacement field. (b) Geometry. (c) GBT discretization.

According to the classical thin-walled beam theory (Vlasov, 1961), the mid-plane displacement field components ($u(x,s)$, $v(x,s)$, $w(x,s)$) are expressed as

$$u(x, s, t) = \Sigma\, u_k(s).\phi_{k,x}(x, t) \quad v(x, s, t) = \Sigma\, v_k(s).\phi_k(x, t) \quad w(x, s, t) = \Sigma\, w_k(s).\phi_k(x, t) \qquad (1)$$

where (i) $(.)_{,x} \equiv d(.)/dx$, (ii) $u_k(s)$, $v_k(s)$ and $v_k(s)$ are functions providing the longitudinal, transverse membrane and transverse flexural displacements characterizing deformation mode k, and (iii) $\phi_k\,(x, t)$ are amplitude functions describing their variation both along the member length $(0 \le x \le L)$ with time t. It is herein assumed that the summation convention applies to subscript k $(k = 1,..., n_d$, where n_d is the number of deformation modes).

In the context of GBT analyses, these deformation modes and the corresponding mechanical properties (i) have a clear structural meaning and (ii) are determined by a systematic procedure named *cross-section analysis*. The complexity of this task depends on the type of cross-section intended to be analyzed (open/closed, branched/unbranched). Following the methodology proposed by Dinis *et al.* (2006) specifically for arbitrarily "branched" open cross-sections (*i.e.*, whose bifurcation nodes are shared by more than two walls), the cross-section analysis of the T-section steel ($E=210GPa$, $\nu=0.3$, $\rho=7.8t/m^3$) member with the cross-section geometry shown in Fig. 1(a) and the discretization shown in Fig. 1(c) involves 6 independent natural nodes, 2 dependent natural nodes and 11 intermediate nodes, leading to a set of 21 deformation modes: **1-4** are the classical rigid body modes (axial extension, major and minor axis bending and torsion), **5-6** are distortional modes and **7-21** are local modes. The twelve most relevant in-plane deformed configurations are shown in Fig. 2. Depending on the particular problem under consideration, it is possible to select any sub-set of deformation modes (of dimension n_d)

to be used in the GBT problem solution, thus leading to a reduction in the number of degrees of freedom involved.

The next step consists of performing the *member analysis*. This procedure comprises the specifications of the member length, loading and end support conditions, in order to solve the differential equilibrium equation system, which may be obtained by employing a suitable variational principle, such as Hamilton's principle.

In the context of member first-order (geometrically linear) analysis, the GBT system of equilibrium equations (one per deformation mode), expressed in terms of the modal amplitude functions, is given by (Silvestre, 2005):

$$C_{ik}\,\phi_{k,xxxx} - D_{ik}\,\phi_{k,xx} + B_{ik}\,\phi k - \boldsymbol{a_B}\,\lambda W_p^{\,0}\,X_{pik}\,\phi_{k,xx} - \boldsymbol{a_V}\,\omega^2\,(R_{ik}\,\phi_k - Q_{ik}\,\phi_{k,xx} = 0 \qquad (2)$$

and the boundary conditions are written as:

$$(W_i^{\tau} + \boldsymbol{a_B}\,W_p^{\,0}\,X_{pik}\,\phi_{k,x} - \boldsymbol{a_V}\,\omega^2\,Q_{ik}\,\phi_{k,x})\delta\phi_{i,x}\,\big|_0^L = 0 \qquad W_i^{\sigma}\,\delta\phi_{i,x}\,\big|_0^L = 0 \qquad (3)$$

where (i) $i \geq 1,\ 1 \leq p \leq 4\ e\ k = 1,\ldots,\ n+1,$ (ii) $\phi_k(x)$ are the problem unknowns, (iii) W_p^0 is the pre-buckling internal forces and moments (uniform along the member length) acting on the member that can be either (a) axial compressive forces $(W_1^0=N)$, (b) major $(W_2^0=M_I)$ or minor axis bending moments $(W_3^0=M_{II})$, (c) bi-moments $(W_4^0=B)$ or (d) any combination of them, (iv) W_i^{σ} and W_i^{τ} are generalized internal forces due to the normal and shear stress related to deformation mode k and acting at the member end sections, (v) λ is an applied load parameter and (vi) ω is a frequency parameter, concerning the member harmonic free vibration.

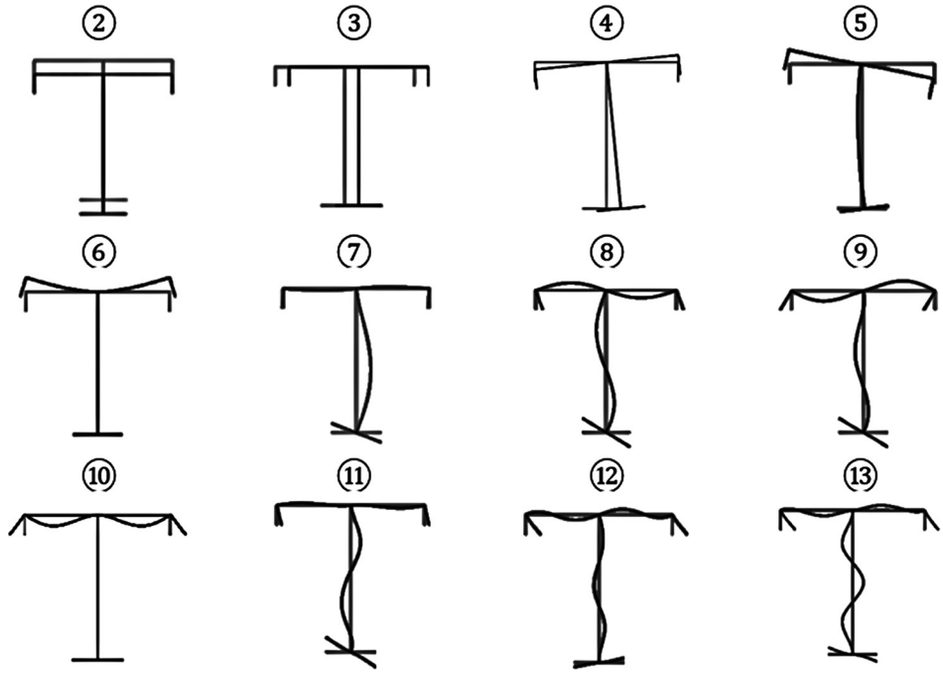

Figure 2
T-section: in-plane shapes of the twelve most relevant deformation modes.

The solution to buckling or vibration problem yields on determining the corresponding eigenvalues (buckling loads or natural frequencies) and eigenvectors (buckling or vibration mode shapes) – the latter provide the coefficients of the modal amplitude functions. With this purpose, if one makes (i) $\boldsymbol{a_B} = \boldsymbol{1}$ and $\boldsymbol{a_v} = \boldsymbol{0}$, (ii) $\boldsymbol{a_B} = 0$ and $\boldsymbol{a_v} = \boldsymbol{1}$ or (iii) $\boldsymbol{a_B} = \psi\ (0 \leq \psi \leq 1)$ and $\boldsymbol{a_v} = \boldsymbol{1}$, Eqs. (2) and (3) define, respectively, the (i) buckling analysis, (ii) free vibration analysis of load-free members and (iii) free vibration analysis of loaded members (*i.e.*, acted by generalized internal forces W_p^0). In the last case, note the value of W_p^0 is known *a priori* and ω^2 are the problem eigenvalues. The tensorial quantities appearing in Eqs. (2) and (3) are given by the expressions:

$$C_{ik} = \frac{E}{(1-\nu^2)}\int_S e u_i u_k ds + \frac{E}{12(1-\nu^2)}\int_S e^3 w_i w_k ds \qquad (3a)$$

$$B_{ik} = \frac{E\,e^3}{12(1-\nu^2)}\int_S w_{i,ss}\,w_{k,ss}\,ds \qquad (3b)$$

$$D_{ik} = \frac{G\,e^3}{3}\int_S w_{i,s}\,w_{k,s}\,ds - \frac{\nu\,E\,e^3}{12(1-\nu^2)}\int_S (w_i\,w_{k,ss} + w_k\,w_{i,ss})\,ds \qquad (3c)$$

$$X_{jik} = \frac{E}{(1-\nu^2)}\int_S e u_j (v_i v_k + w_i w_k)\,ds \qquad (3d)$$

$$Q_{ik} = \rho e \int_S u_i u_k ds + \int_S \frac{\rho e^3}{12} e^3 w_i w_k ds \quad (3e)$$

$$R_{ik} = \rho e \int_S (v_i v_k + w_i w_k)\, ds + \int_S \frac{\rho e^3}{12} w_{i,s} w_{k,s} ds \quad (3f)$$

where E, G, ν and ρ are the Young's modulus, shear modulus, Poisson's ratio and mass density, respectively. It is worth noting that (i) C_{ik}, D_{ik} and B_{ik} are linear stiffness matrices. The components of C_{ik} and D_{ik} represents the warping displacements and torsional rotations, while B_{ik} stems from local deformations (wall bending and distortion), (ii) X_{jik} are geometric stiffness matrices associated with the acting axial normal stress resultants W_p^0, (iii) Q_{ik} and R_{ik} are mass matrices that account for the influence of the inertia forces on the out-of and in-plane cross-section displacements.

At this point, it should be mentioned that the GBT-based vibration/buckling results presented herein have been obtained through the application of the Galerkin method (only simply supported members are considered, *i.e.*, members with locally and globally pinned and free-to-warp end sections), which means that the exact solutions of Eqs. (2)-(3) are sinusoidal functions

$$\phi_{k,x} = d_k \sin\left(\frac{n_s \pi x}{L}\right) \quad (4)$$

where d_k is the amplitude associated with deformation mode k and n_s is the vibration/buckling mode number of the solution.

The following sections illustrate and discuss the vibration behavior of load-free and loaded T-section members with (i) the cross-section depicted in Fig. 1(b), (ii) the discretization shown in Fig. 1(b) and (iii) the particular dimensions of $b_w = 150$ *mm* (web width), $b_s = 150$ *mm* (top flange width), $b_i = 50$ *mm* (bottom flange width), $s = 20$ *mm* (stiffener width) and $e = 3$ *mm* (wall thickness) – the influence of the applied loadings (uniform major-axis bending moment) is assessed in terms of (i) the fundamental frequency variation and (ii) the change in the corresponding vibration mode shape.

3. Load-free vibration behavior

The curve displayed in Fig. 3(a) shows the variation of the load-free T-section first three natural frequencies ($\omega_1 \equiv \omega_f$, ω_2 and ω_3, where ω_f is the fundamental frequency) for members exhibiting $L \leq 1000$ *cm* – for clarity purposes, both axes are expressed in logarithmic scale. Moreover, Fig. 3(b) presents the GBT modal participation diagram concerning the member fundamental vibration mode shapes – this diagram provides the contribution of each deformation mode to a deformed configuration mode nature. Finally, Figs. 3(c_1)-(c_2) show the GBT and ABAQUS fundamental vibration mode shapes of members with L=20*cm* and L=150*cm*.

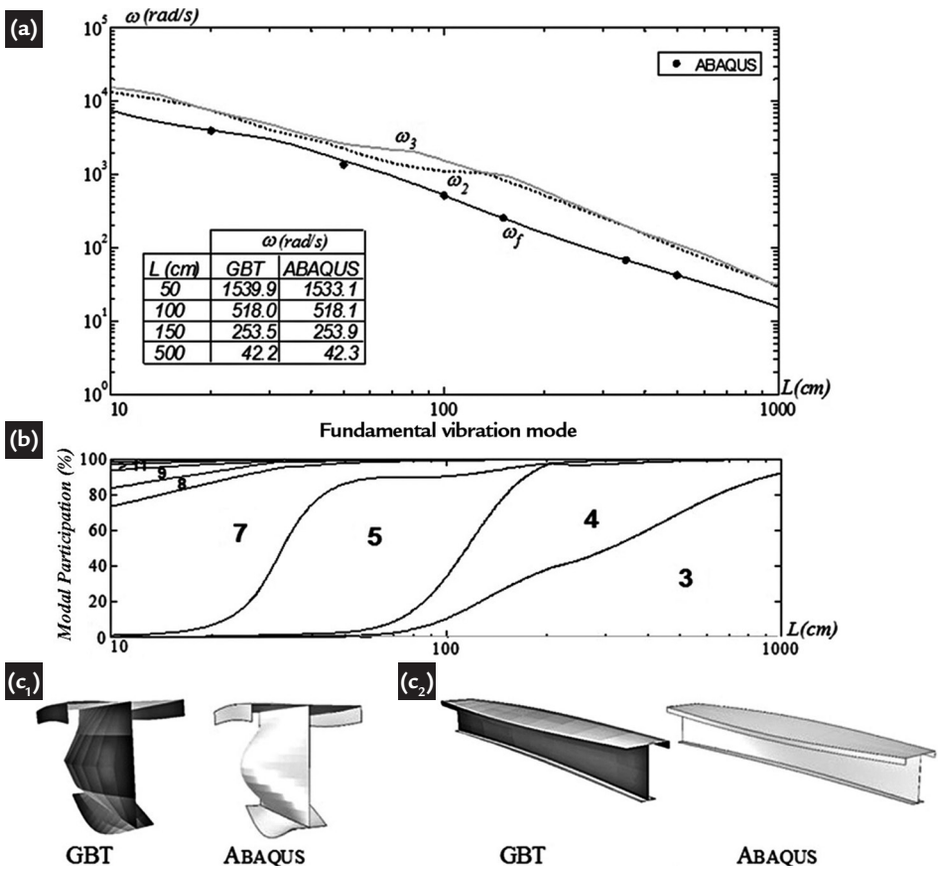

Figure 3
Load-free member vibration behavior: (a) variation of ω_f with L, (b) GBT modal participation diagram in the fundamental (load-free) vibration mode and (c) vibration mode configurations for (c_1) L=20*cm* and (c_2) L=150*cm*.

These results prompt the following remarks:

(i) The curves $\omega_1(L)$, $\omega_2(L)$ and $\omega_3(L)$ exhibit no local minima. As the length increases, all of them decrease monotonically and tends to null fundamental frequency values.

(ii) Regardless of the member length, the fundamental frequency ω_f is always associated with single half-wave (local or global) vibration modes (*i.e.,* $n_s = 1$).

(iii) For $L \leq 20$ cm, the modal participation diagram reveals that the fundamental vibration modes involve only local deformation modes ($L \equiv 7 + 8 + 9 +$ bit of $11 + 12 + 13$) – the number of deformation modes involved is relatively high to annul the top flange deformation.

(iv) For $45 \leq L \leq 100$ cm, the participation of the distortional mode ($D \equiv 5$) becomes dominant, despite small contributions of local ($L \equiv 7$) and global (flexural torsional $FT \equiv 4 + 3$) modes. Moreover, the GBT modal composition also indicates the predominance of mixed modes, which combine two main natures: $LD \equiv 7 + 5 +$ bit of $8 + 9$ ($20 \leq L \leq 45$ cm) and $DFT \equiv 5 + 4 + 3$ ($100 \leq L \leq 200$ cm). It also can be noted that there is a smooth transition between the LD and DFT modes.

(v) For long members ($L \geq 200$ cm), the fundamental vibration mode shape is purely flexural-torsional ($FT \equiv 4 + 3$).

(vi) There is an excellent agreement between the GBT-based results and the values yielded by ABAQUS shell finite element analysis (the differences always below 0.5%) – however, note that the latter involve 2000-26600 d.o.f., while the former require only 21. In order to enable a quantification of this agreement, the table in Fig. 3(a) shows the variation of ω_f with L.

4. Loaded member vibration behavior

The vibration behavior of loaded T-section members acted by uniform major-axis bending moment (the applied moments cause compression on the top flange – the most probable loading case) is addressed next. The simply supported beam buckling behavior is first analyzed, since his knowledge is indispensable to assess the loaded member vibration behavior.

4.1 Beam buckling behavior

The curves presented in Fig. 4(a) concern variation, with the beam length L (in logarithmic scale), of the bifurcation moments ($M_{b.1}$, $M_{b.2}$, and $M_{b.3}$) associated with single, two and three (n_s = 1-3) wave buckling modes, as well (ii) the critical buckling moment M_{cr} = min ($M_{b.1}$, $M_{b.2}$, $M_{b.3}$, ..., $M_{b.ns}$, where $n_s = \infty$). The modal participation diagrams for single-wave (Fig. 4(b)) and critical (Fig. 4(c)) buckling modes provide valuable information about the contribution of the relevant GBT deformation modes in the beam buckling behavior and the evolution of the number of half-waves with the length.

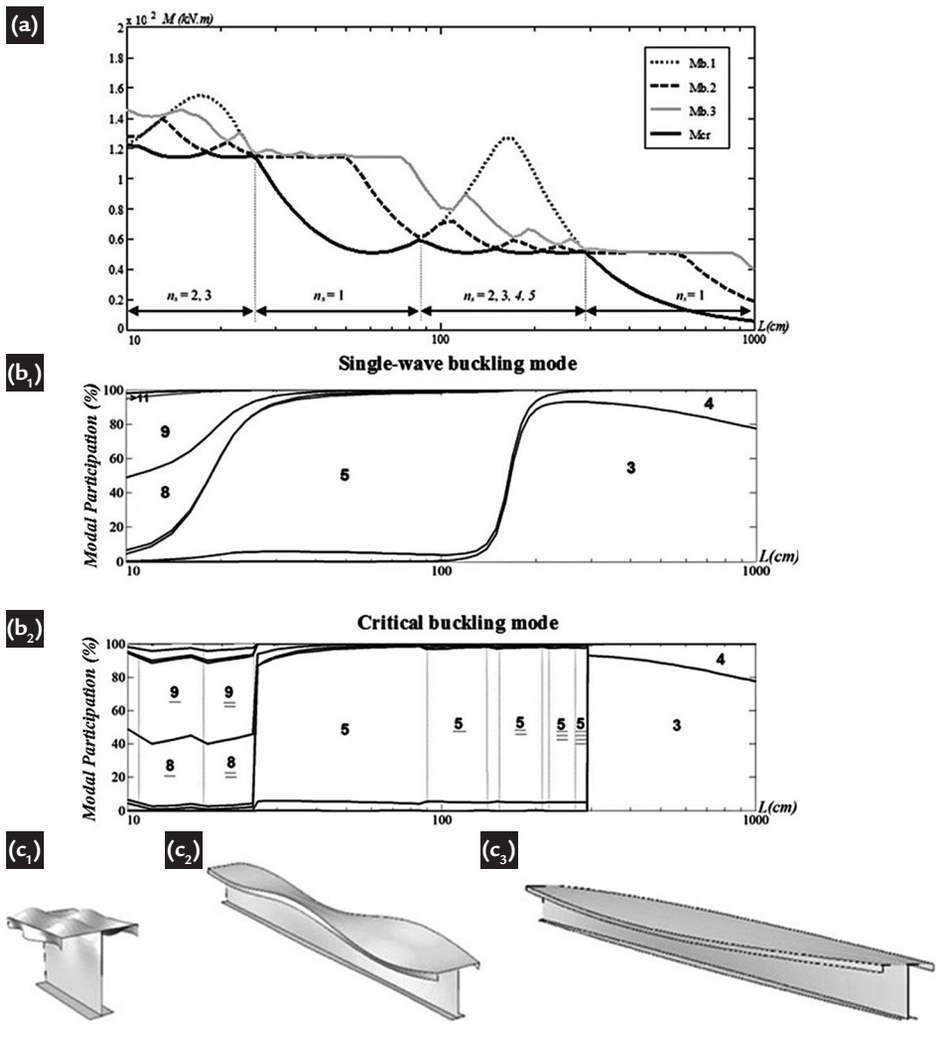

Figure 4
Beam buckling behavior: (a) Variation of $M_{b.1}$, $M_{b.2}$, $M_{b.3}$ and M_{cr} with L, (b) GBT modal participation diagrams in (b_1) single-wave and (b_2) critical buckling modes and (c) ABAQUS buckling mode configurations for (c_1) L=20cm, (c_2) L=150cm and (c_3) L=500cm

Note that, in order to access the number of half-waves associated with the participation of a given deformation mode, the number identifying this mode is either not underlined (single-wave), underlined once (2 waves) or underlined twice (3 waves). The subsequent vertical lines separate length ranges connected to critical buckling modes exhibiting a growing number of half-waves. Finally, Figs. 4(c_1)-(c_3) depict the ABAQUS critical buckling modes for beams with L=20, 150 and 500cm. These buckling results lead to the following comments:

(i) The critical buckling curve exhibits three distinct zones, corresponding to (i_1) 1-3 wave local buckling ($L \leq 25$ cm), (i_2) 1-5 distortional buckling wave ($25 < L \leq 291$ cm) and (i_3) single-wave global (flexural-torsional) buckling ($L > 291$ cm). It only differs from its single-wave counterpart for (i_1) $10 \leq L \leq 25$ cm (2–3 wave local buckling) and (i_2) $85 \leq L \leq 291$ cm (2–5 wave distortional buckling).

(ii) The single-wave buckling curve exhibits two local minima at $L \approx 15$ cm ($M_{cr.L} \cong 114.1$ kN.m) and $L \approx 60$ cm ($M_{cr.D} \cong 50.9$ kN.m), (ii_1); the former corresponding to a local buckling mode that combines modes 7, 8, 9, 11, 12 and 13, and (ii_2) the latter associated with a distortional buckling mode combining modes 5 (predominant) and a bit of 7 and 8.

(iii) Although, the curve $M_{cr}(L)$ does not coincide with $M_{b.1}(L)$ in all its extension, the critical beam buckling modes combines exactly the same set of GBT deformation modes participating in single-wave ones. The only difference resides in the fact that the number of waves associated with some of these critical modes changes for certain range lengths. In this case, the critical buckling modes exhibit two ($11 \leq L \leq 17$ cm and $90 \leq L \leq 140$ cm), three ($18 \leq L \leq 25$ cm and $150 \leq L \leq 210$ cm), four ($220 \leq L \leq 270$ cm) and five ($280 \leq L \leq 291$ cm) waves.

(iv) Finally, it is worth noting that the single half-wave T-section beam buckling modes (Fig. 4(b_1)) and load-free member fundamental vibration modes (Fig. 3(b)) are not identical. Indeed, although combining exactly the same set of GBT deformation modes participating significant differences occurs throughout the whole lengths range – note that these differences were not observed in a previous thin-walled loaded member vibration study involving lipped channel columns (Silvestre and Camotim, 2006).

4.2 Loaded beam vibration behavior

The local, distortional and global vibration behavior of T-section members acted by uniform major-axis bending moment is addressed next. The analyses are carried out for beams subjected to several loading levels, defined as percentages of the corresponding critical bifurcation values, *i.e.*, $\alpha = M/M_{cr}$, where $0 \leq \alpha \leq 1$. Seven levels of load are considered, namely $\alpha = 0.25$, 0.50, 0.75, 0.90, 0.95, 0.99, and the influence of the loading is assessed through the (i) fundamental frequency values ($\omega_{f.M}$) and (ii) vibration mode shapes – in order to clarify that influence, the load-free member vibration curve ($M = \alpha = 0 - \omega_{f.0}$ curve), already shown in Fig. 3(a), are also presented.

The curves depicted in Fig. 5 display the variation of $\omega_{f.M}$ with the length L, for members vibrating under the action of $\alpha\, M_{cr}$ – for clarity purposes, (i) this figure also depicts the L values for which the critical buckling mode exhibit a number of half-waves greater than 1 (recall that the curve $M_{cr}(L)$ was plotted in Fig. 4(a)) and (ii) both axes are expressed in logarithmic scale. The modal participation diagrams shown in Figs. 6(a)-(f) enable to assess the influence of the applied load levels (α = 0.25, 0.50, 0.75, 0.90, 0.95, 0.99) on the fundamental vibration mode shapes.

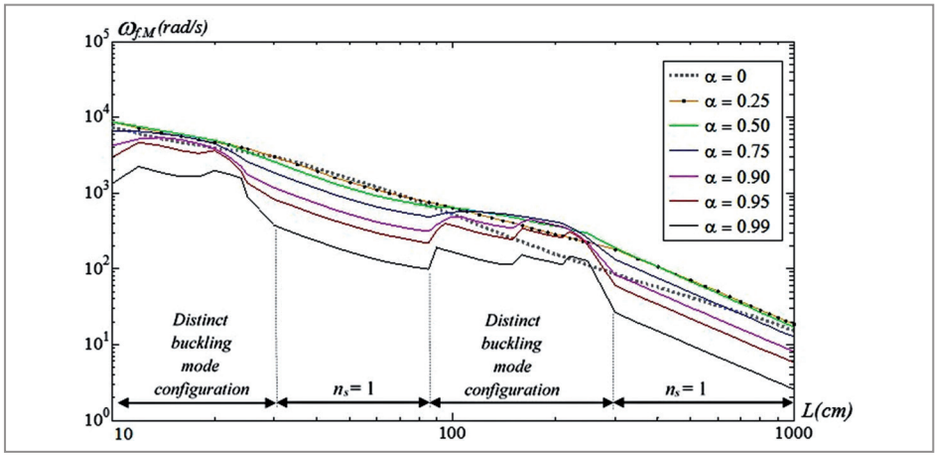

Figure 5
Beam vibration behavior: variation of the fundamental frequency $\omega_{f.M}$ with α and L.

The observation of these vibration results leads to the following comments:

(i) As expected, the $\omega_{f.M}$ curves (i_1) vary considerably with L, (i_2) moves down as α increases, (i_3) remain parallel and fairly close to the initial load-free one (as long the column vibration mode associated with $\omega_{f.M}$ exhibits a single half-wave) and (i_4) the frequency drop is more pronounced when the applied moment level approaches its critical value ($\alpha = 0.99$).

(ii) Moreover, when $M_{cr} \neq M_{b.1}$ ($11 \leq L \leq 27$ cm and $86 \leq L \leq 299$ cm), the shapes of the curves become visibly different as the value of α increases. Indeed, the number of half-waves associated with the curves $\omega_{f.M}$ depends on the percentage of applied bending moment (never exceeding the number of the critical buckling mode – in this case, $n_s \leq 5$).

(iii) The fundamental vibration mode shape is considerably altered even by the presence of small applied moments (e.g., $\alpha = 0.25$) – see the modal participation diagrams presented in Figs. 3(b) and 6(a). On the other hand, for $\alpha \geq 0.90$ the vibration mode, shapes change drastically, approaching their critical buckling mode counterparts – compare Figs. 4(b_2) and 6(f)).

(iv) However, the T-section loaded member vibration behavior exhibit an uncommon feature, namely the fact that the $\omega_{f.0}$ curve does not remain as the upper curve for the whole beam length.

Indeed, only for $30 \leq L \leq 86$ cm the $\omega_{f,M}$ curves exhibit this characteristic, which was observed in previous thin-walled loaded members vibration studies involving lipped channel columns (e.g., Silvestre and Camotim, 2006).

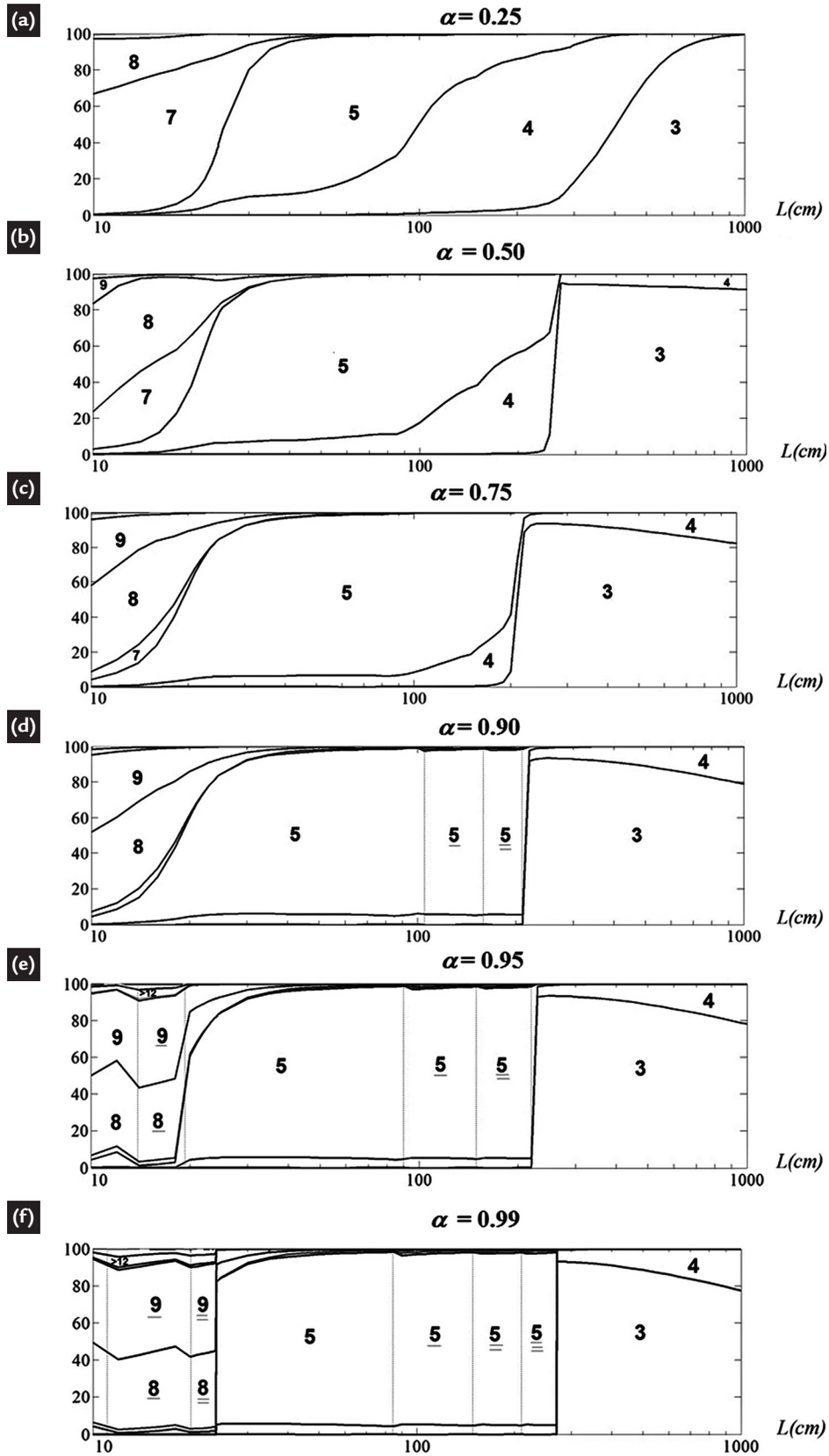

Figure 6
GBT modal participation in the beam fundamental vibration mode for (a) $\alpha = 0.25$, (b) $\alpha = 0.50$, (c) $\alpha = 0.75$, (d) $\alpha = 0.90$, (e) $\alpha = 0.95$ and (f) $\alpha = 0.99$.

In order to acquire further and deeper insight on the influence of the loading level on the vibration behavior of beams, namely providing the explanation for the unexpected vibration behavior of the T-section members, the variation of the fundamental frequency ratio $\omega_{f,M}/\omega_{f,0}$ with α for members with (i) L=60 cm (length inside the $30 \leq L \leq 86$ cm interval mentioned above), (ii) L=120 cm and (iii) L=180 cm is plotted in Fig. 7. The analyses are carried out for beams subjected (i) to uniform positive or negative major axis bending (i.e., $-1 \leq \alpha \leq 1$), and (ii) to twelve

load levels (α = ±0.25, ±0.50, ±0.75, ±0.90, ±0.95, ±0.99). This figure also includes several $\omega_{f.M}/\omega_{f.0}$ values, obtained through ABAQUS shell finite element analyses and used to validate the GBT-based results.

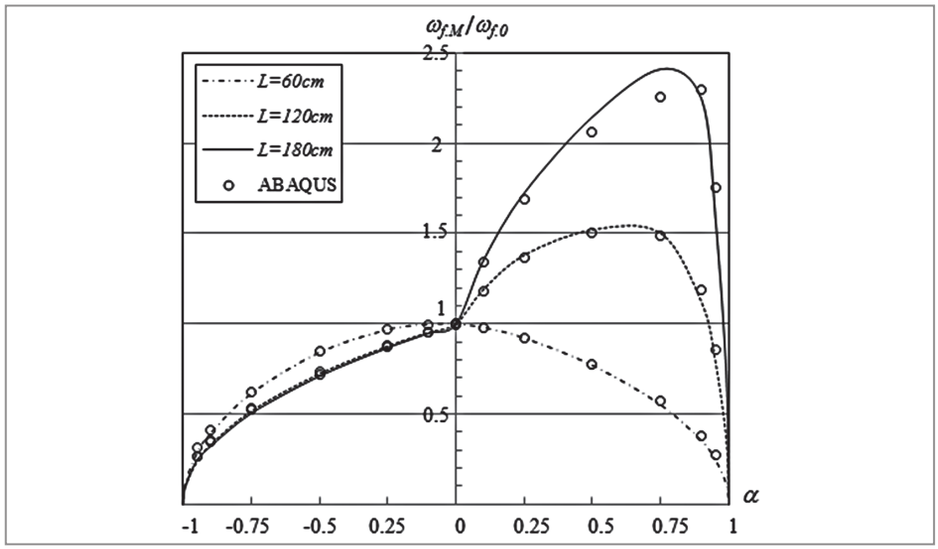

Figure 7
Variation of the ratio $\omega_{f.M}/\omega_{f.0}$ with α for beams with L = 60, 120 and 180 cm.

As for Figs. 8(a)-(e), they present the GBT and FEM-based vibration mode shapes for members with L = 60 cm and (i) α = 0 (load-free vibration), (ii) α = ±0.75 and (iii) α = ±0.95. Finally, Figs. 9(a)-(c) and 10(a)-(c) show similar vibration mode shapes for three loading cases (α=0, 0.75 and 0.95) – they correspond to members with lengths equal to L = 120 cm (Fig. 9) and L = 180 cm (Fig. 10).

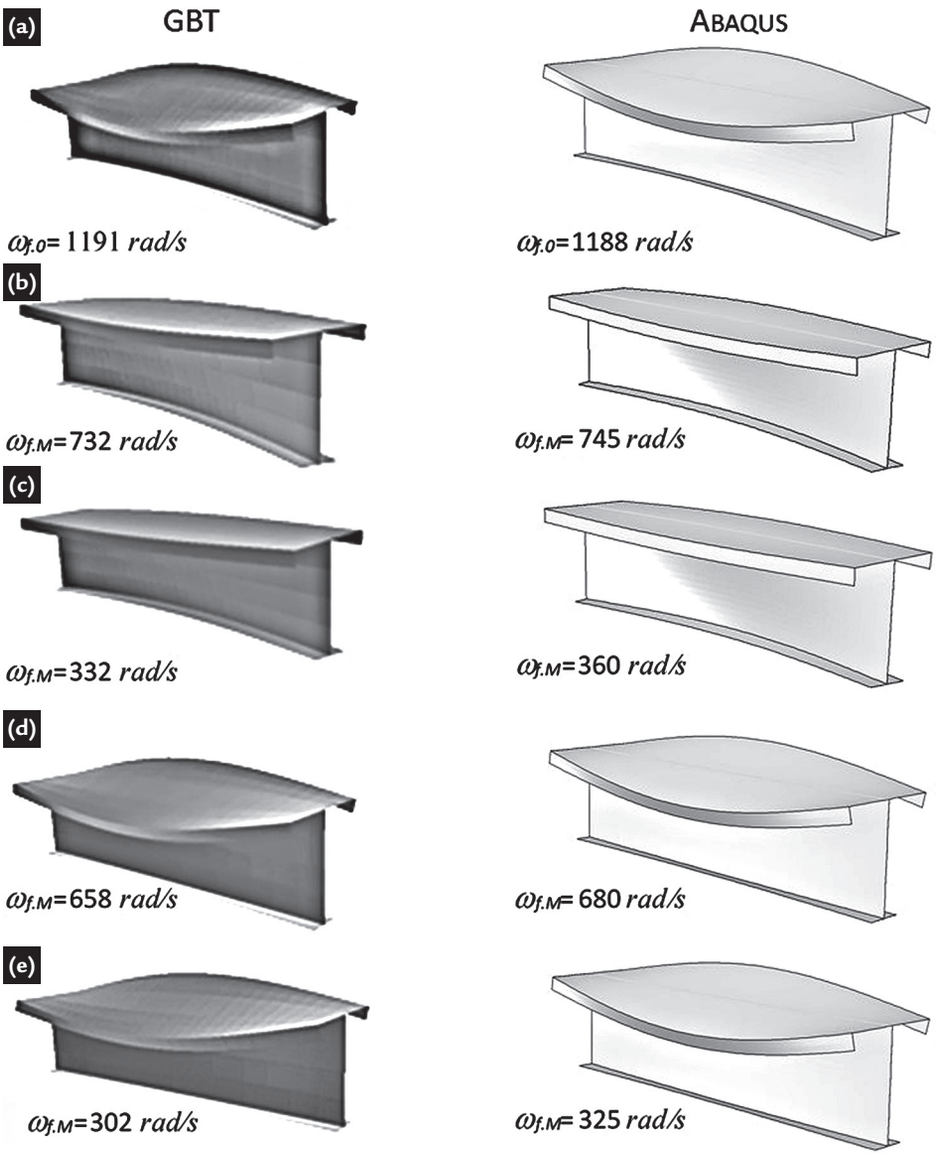

Figure 8
GBT and ABAQUS vibration mode shapes for L = 60 cm and (a) α = 0 (load-free vibration), (b) α = −0.75, (c) α = −0.95, (d) α = 0.75 and (e) α = 0.95.

The observation of these results leads to the following conclusions:

(i) First of all, there is a fairly good correlation between the fundamental frequency values and vibration mode shapes obtained through ABAQUS shell finite element and GBT-based analyses, which fully validates the latter – the differences on the fundamental frequency values increase with α: (i_1) they are minor for small applied moments (less than 4% for $-0.50 \leq \alpha \leq 0.50$, ($i_2$) increases to 7% for $-0.90 \leq \alpha \leq 0.90$, and ($i_3$) reaches 10% for higher applied moments (the $\omega_{f.M}$ increase is due to the fact that the load-free vibration mode shape is very different from the loaded member one – the former a *flexural-torsional* mode, the latter a *distortional-torsional* one (**5** + a bit of mode **4**). Moreover, note that (v_1) T-section is very asymmetric relative to the major-axis and (v_1) positive moments originate tractions on the bottom flange, which increase the stiffness of the weak part of the cross-section).

(ii) The $\omega_{f.M}/\omega_{f.0}$ curves concerning L = 60 cm beams under positive major-axis bending ($\alpha > 0$) are relatively similar to their negative counterparts ($\alpha < 0$) – the fundamental frequency of the loaded beams (ii_1) are always lower than their natural frequency and (ii_2) tend to zero as α increase to ± 1.0. Moreover, the curve of the beam under negative applied moments always lie above the positive ones – the latter loaded member vibration mode is more akin to the load-free one (see Fig. 8).

(iii) The fundamental frequencies of the other two beams (L = 120 and 180 cm) under positive major-axis bending are also lower than $\omega_{f.0}$. However, note that both curves lie above to their L = 60 cm counterpart – the GBT provides the explanation for the distinct vibration behaviors exhibited by this groups of columns. Indeed, with two distinct load-free vibration modes: (iii1) local-distortional-torsional one (4+5 + a bit of mode 7), for L = 60 cm beam, and (iii_2) flexural-torsional ones (4+3), for L = 120 and 180 cm beams.

(iv) Finally, the curves concerning the L = 120 and 180 cm beams under positive major-axis bending ($\alpha > 0$) exhibit $\omega_{f.M}$ values that may be significantly higher than the natural frequencies. Indeed, those values may increase up to (iv_1) 1.5 times (L = 120 cm) and (iv_2) 2.4 times $\omega_{f.0}$ (L = 180 cm) – the increase is connected to the maximum number of longitudinal half-waves to be exhibited by the (sinusoidal) vibration mode: two for L = 120 cm beam, three for the L = 180 cm one (see Fig. 9 and Fig. 10).

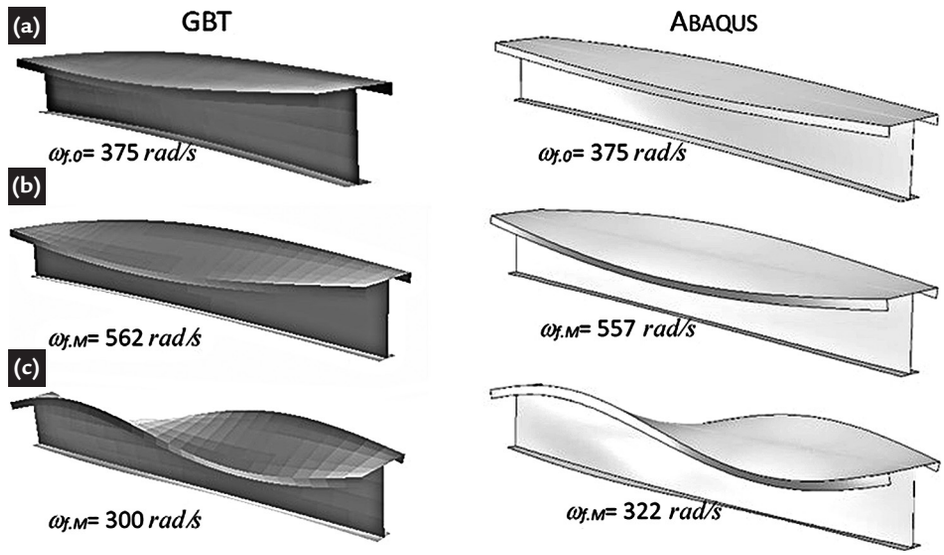

Figure 9
GBT and ABAQUS vibration mode shapes for L = 120 cm and (a) α = 0 (load-free vibration), (b) α = 0.75 and (c) α = 0.95.

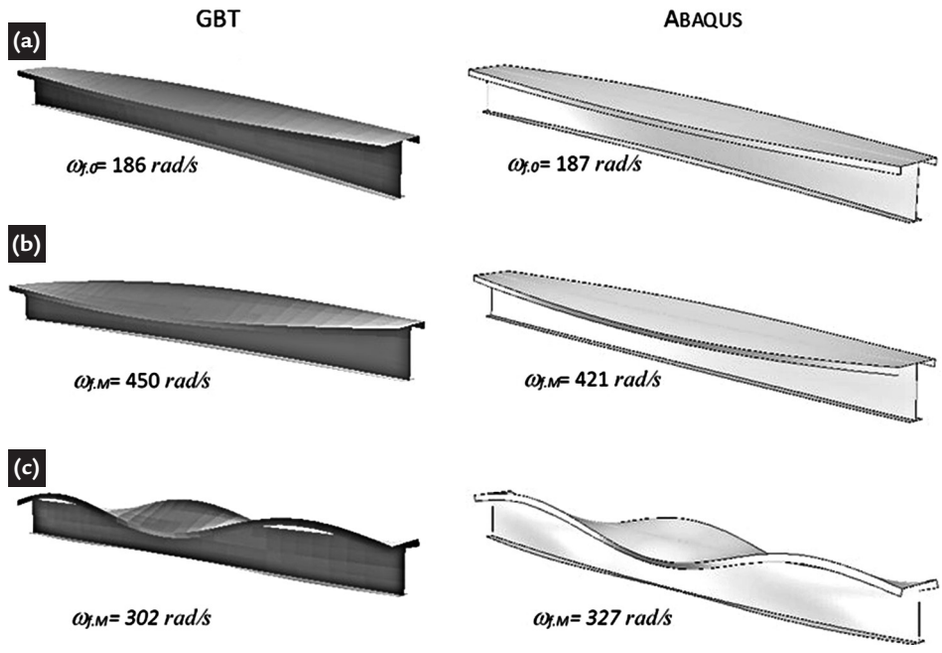

Figure 10
GBT and ABAQUS vibration mode shapes for L = 180 cm and (a) α = 0 (load-free vibration), (b) α = 0.75 and (c) α = 0.95.

5. Conclusions

This article reported an investigation, carried out by means of analyses based on the Generalized Beam Theory (GBT), dealing with the influence of uniform major-axis bending moment (compression on the top flange) on the fundamental vibration behavior of thin-walled T-section (with unequal flanges) members. Various loading levels, expressed as percentages of the member critical buckling moments (i.e., $\alpha = M/M_{cr}$, where $0 \leq \alpha \leq 1$), were considered and the load-sensitivities of the member's fundamental frequency and vibration mode shape (taking advantage of the GBT modal features) were assessed through the comparison relative to the load-free case. Some GBT-based results (fundamental frequency and vibration mode shapes) were validated by means of values and mode shapes provided by numerical analyses performed with the code ABAQUS (Simulia, 2008). The analysis of the GBT-based results obtained, led to the following main conclusions:

(i) As expected, the load-free member vibration behavior is characterized by the fact that the fundamental frequency is always associated with single-wave (local, distortional or global) vibration modes, regardless of the member length – the mode is a distortional-flexural-torsional one for intermediate-to-long members, progressively fading the participation of the symmetric distortional mode as the member length grows.

(ii) Moreover, (ii_1) the beam single-wave buckling $P_{b.1}$ vs. L curve and the load-free fundamental vibration $\omega_{f.0}$ vs. L curve exhibit significant differences (e.g., the latter has no local minima) and (ii_2) the single half-wave beam buckling modes and load-free member fundamental vibration modes are not identical. Indeed, although combining exactly the same set of GBT deformation modes participating significant differences occurs throughout the whole lengths range – differences not observed in a previous thin-walled members vibration studies involving lipped channels (Silvestre and Camotim, 2006).

(iii) The effect of applied bending moments on the member vibration frequency ($\omega_{f.M}$) increases with the value of moment. Indeed, the $\omega_{f.M}$ vs. L curves (i_1) vary considerably with L, (i_2) moves down as α increases, (i_3) remain parallel and fairly close to the initial load-free one (as long the column vibration mode associated with $\omega_{f.M}$ exhibits a single half-wave), (i_4) the frequency drop is more pronounced when the applied moment level approaches its critical value ($\alpha = 0.99$) and (i_5) the vibration mode shape modifies significantly and approaches their critical buckling mode counterparts (i.e., same shape and number of half-waves).

(iv) However, the T-section loaded member vibration behavior exhibits an uncommon feature, namely the fact that the $\omega_{f.0}$ curve does not remain as the upper curve for the whole beam length – this characteristic was observed in previous thin-walled loaded member vibration studies involving lipped channel columns (Silvestre and Camotim, 2006). The increase is due to the fact that the load-free vibration mode shape is very different from the loaded member one.

Acknowledgements

The authors would like to convey their thanks to CNPq/Brazil.

References

BEBIANO, R., SILVESTRE, N., CAMOTIM, D. Local and global vibration of thin-walled members subjected to compression and non-uniform bending. ***Journal of Sound and Vibration,*** v. 315, n. 3, p. 509-535, 2008.

BEBIANO, R., CAMOTIM, D. GONÇALVES, R.M. Local and global vibration analysis of thin-walled members subjected to internal forces – application of Generalised Beam Theory. In: DIMITROVOVÁ, Z. et al. (Eds.). In: INTERNATIONAL CONFERENCE ON VIBRATION PROBLEMS, 11. Lisbon, Portugal, 9-12 Sept. 2013.

BORBÓN, F. DE, AMBROSINI, D. On free vibration analysis of thin-walled beams axially loaded. ***Thin-Walled Structures,*** v. 48, n. 12, p. 915-920, 2010.

CAMOTIM, D., BASAGLIA, C., SILVA, N.F., SILVESTRE, N. Numerical analysis of thin-walled structures using Generalised Beam Theory (GBT): recent and future developments. ***Computational Technology Reviews,*** n. 1, p. 315-354, 2010.

CAMOTIM, D., SILVESTRE, N., BEBIANO, R. GBT-based local and global vibration analysis of Thin-Walled Members. In: SHANMUGAN, N.E. WANG, C. M. (Eds.). ***Analysis and Design of Plated Structures: Dynamics.*** England: CRC Press, n. 1, p. 36-74, 2007.

DINIS, P.B. CAMOTIM, D., SILVESTRE, N. GBT formulation to analyse the buckling behavior of thin-walled members with arbitrarily 'branched' open cross-sections. ***Thin-Walled Structures,*** v. 44, n. 1, p. 20-38, 2006.

JOSHI, A., SURYANARAYAN, S. Unified analytical solution for various boundary conditions for the coupled flexural-torsional vibration of beams subjected to axial loads and end moments. ***Journal of Sound and Vibration,*** v. 129, n. 2, p. 313-326, 1989.

JOSHI, A., SURYANARAYAN, S. Iterative method for coupled flexural-torsional vibration of initially stressed beams. ***Journal of Sound and Vibration,*** v. 146, n. 1, p. 81-92, 1991.

KASHANI, M.T.T., JAYASINGHE, S., HASHEMI, S.M. On the flexural-torsional

vibration and stability of beams subjected to axial load and end moment. ***Shock and Vibration,*** 2014.

MAGNUCKA-BLANDZI, E. Critical state of a thin-walled beam under combined load. ***Applied Mathematical Modelling,*** v. 33, n. 7, p. 3093-3098, 2009.

MOHRI, F., BOUZERIRA, C., POTIER-FERRY, M. Lateral buckling of thin-walled beam-column elements under combined axial and bending loads. ***Thin-Walled Structures,*** v. 46, n. 3, p. 290-302, 2008.

MOTAMARRI, P., SURYANARAYAN, S. Unified analytical solution for dynamic elastic buckling of beams for various boundary conditions and loading rates. ***International Journal of Mechanical Sciences,*** v. 56, n. 1, p. 60-69, 2012.

OHGA, M., NISHIMOTO, K., SHIGEMATSU, T., HARA, T. Natural frequencies and mode shapes of thin-walled members under in-plane forces. In: SHANMUGAM, N. et al. (Eds.). ***Thin-Walled Structures – Research and Development.*** Elsevier, p. 501-508, 1998.

OKAMURA, M., FUKASAWA, Y. Characteristics of instability of local vibration of thin-walled members under periodic axial forces. ***Structural and Earthquake Engineering (JSCE),*** v. 15, n. 2, p. 215-223, 1998.

PAVLOVIĆ, R., KOZIC, P., RAJKOVIĆ, P., PAVLOVIĆ, I. Dynamic stability of a thin-walled beam subjected to axial loads and end moments. ***Journal of Sound and Vibration,*** v. 301, n. 3-5, p. 690-700, 2007.

SCHARDT, R. Eine Erweiterung Der Technischen Biegetheorie Zur Berechnung Prismatischer Faltwerke. ***Der Stahlbau,*** v. 35, p. 161-171, 1966.

SCHARDT, R., HEINZ, D. Vibrations of Thin-Walled Prismatic Structures Under Simultaneous Static Load Using Generalized Beam Theory. In: BRUHNS, O. T et al. (Eds). ***Structural Dynamics.*** Rotterdam, Balkema Publishers, The Netherlands, p. 921-927, 1991.

SHIH, C.F., CHEN, J.C., GARBA, J. Vibration of a large space beam under gravity effect. ***AIAA Journal,*** v. 24, n. 7, p. 1213-1216, 1986.

SILVESTRE, N. ***Generalised Beam Theory: new formulations, numerical implementation and applications.*** Lisbon: Civil Engineering Department, IST, Technical University of Lisbon, 2005. (Ph.D. Thesis, in portuguese).

SILVESTRE, N., CAMOTIM, D. First-order generalised beam theory for arbitrary orthotropic materials. ***Thin-Walled Structures,*** v. 40, n. 9, p. 755-789, 2002.

SILVESTRE, N., CAMOTIM, D. Vibration behaviour of axially compressed cold-formed steel members. ***Steel and Composite Structures,*** v. 6, n. 3, p. 221-236, 2006.

SILVESTRE, N., CAMOTIM, D. GBT-based local and global vibration analysis of loaded composite open-sections thin-walled members. ***International Journal of Structural Stability and Dynamics,*** v. 6, n. 1, p. 1-29, 2006a.

SILVESTRE, N., CAMOTIM, D. Generalized Beam Theory to analyse the vibration of open-section thin-walled composite members. ***J. Eng. Mech.,*** Special Issue: Stability of Composite Structures, v. 139, n. 8, p. 992–1009, 2012. Simulia Inc., Abaqus Standard, 2008 (version 6.7-5).

TALIMIAN, A., VÖRÖS, G.M. Dynamic stability analysis of a thin-walled beam subjected to a time periodic gradient bending moment. ***Civil Engineering,*** v. 57, n. 2, p. 123-128, 2013.

URBANIAK, M., KUBIAK, T. Local dynamic buckling of C-shape profiles subjected to bending. ***Mechanics and Mechanical Engineering,*** v. 15, n. 1, p. 129-144, 2011.

VERMA, V.K. Vibration of multi-span thin walled beam due to torque and bending moment. ***Advances in Structural Engineering,*** Springer India, p. 215-220, 2015.

VLASOV, V.Z. ***Thin-walled elastic beams.*** Washington: National Science Foundation, 1961.

VO, T.P., LEE, J. Interaction curves for vibration and buckling of thin-walled composite box beams under axial loads and end moments. ***Applied Mathematical Modelling,*** v. 34, n. 10, p. 3142-3157, 2010.

VO, T.P., LEE, J. Free vibration of axially loaded thin-walled composite Timoshenko beams. ***Archive of Applied Mechanics,*** v. 81, n. 9, p. 1165-1180, 2011.

VO, T.P., LEE, S.J. Vibration and buckling of thin-walled composite I-beams with arbitrary lay-ups under axial loads and end moments. ***Mechanics of Advanced Materials and Structures,*** v. 20, n. 8, p. 652-665, 2013.

Received: 4 December 2017 - Accepted: 15 February 2018.